2020

The use of sea sand and sea water in concretes for floating wind farm foundations

Farnell, H.

Farnell, H. (2020) 'The use of sea sand and sea water in concretes for floating wind farm foundations', The Plymouth Student Scientist, 13(1), p. 173-202.
http://hdl.handle.net/10026.1/16510

The Plymouth Student Scientist
University of Plymouth

*The Plymouth Student Scientist, 2020, **13**, (1), 173-202*

The use of sea sand and sea water in concretes for floating wind farm foundations

Henry Farnell

Project Advisor: Shanshan Cheng, School of Engineering, Computing and Mathematics (Faculty of Science and Engineering), University of Plymouth, Drake Circus, Plymouth, PL4 8AA

Abstract

The object of this paper was to investigate whether a marine durable concrete could be produced that could ultimately be used in floating wind farm foundations to reduce long term costs. It was investigated if sea water and sea sand were a suitable alternative to sand and fresh water in concrete alongside the use of CFRP (Carbon fibre reinforced polymer) as a replacement for steel. Sea water and sea sand concrete was produced alongside fresh water and sea sand concrete. The compressive and tensile performance of the two concretes were tested and compared at 7, 14 and 28 days. Additionally, the flexural performance of CFRP reinforced concrete beams were tested at 28 days. It was found that the use of sea water produced an increase in performance of compressive and tensile strength at 7, 14 and 28 days compared with fresh water. For these tests, increases of 7.3 and 6.4% respectively were found from the sea water concrete at 28 days. It was also found that the flexural strength of sea water concrete was 18.3% higher than fresh water concrete. However, reliability of the flexural test results for fresh water concrete was low and so more testing would be needed to reliably confirm this. In conclusion, the findings show that if using CFRP as a replacement for steel reinforcement in concrete, the use of sea water over fresh water would be beneficial and provide considerable performance gains.

Introduction

WWAP (2018) estimates global water demand will rise to 6000km^3 by 2050. This is an increase of 30% from current usage estimates of 4600 km^3 per year. Ridoutt and Pfister (2010) state that one billion people do not have access to clean drinking water. There is also increasing pressure on fresh water supply due to rising population, climate change etc. In addition, Solidia Technologies (2018) states "overall water consumed annually during OPC-based concrete production is estimated to be between 2.15 to 2.6 billion tons". This doesn't include water also required in the production process which Miller, Horvath and Monteiro (2018) claim to be 16.6km^3 annually based on 2012 concrete consumption values. Clearly, there is already a huge strain on the global fresh water supply, a significant proportion of which can be attributed to concrete production.

Furthermore, it is estimated that yearly global sand consumption is as high as 20 billion tonnes, the second most used natural resource, second only to fresh water (Tweedie, 2018). Half of this is estimated to be used in concrete production. Sand reserves are declining, and illegal sand mining has become a global problem. Additionally, the world is looking to move from oil and gas to renewable energy sources. One alternative is wind energy. Currently offshore wind farms are built in shallow waters where the foundations can be built on the seabed. Shallow waters are limited, and furthermore deeper waters offer more consistent and stronger winds, reduced visual pollution and less interference with shipping lanes. However, wind farms in deeper water are currently too expensive and so one alternative to this is to develop floating wind farm foundations. "The global market for such turbines is potentially enormous, depending on how low we can press costs" said Gjorv (2009). A marine durable concrete would reduce maintenance and increase life expectancy leading to long term savings.

To produce a marine durable concrete, it is possible that carbon fibre could be used for the reinforcement. It could be assumed that carbon fibre would be resistant to the corrosion normally associated with steel reinforcement in concrete. Therefore, could standard sand and fresh water be replaced with sea sand and sea water, hence reducing the pressure on these highly in demand materials whilst also reducing costs and environmental impact.

Methodology

Mix Design

Cement

Hanson High Strength cement, class CEM I 52.5N was used. This was chosen due to being widely available in the lab.

Sand

Marine dredged sand was used. Initial tests showed this contained very little salt content so was likely washed with fresh water rather than naturally drained. The sand was oven dried before use. A sieve analysis was also carried out to grade the sand. A 250g sample of sand was added to the sieves seen in Figure 1 and sieved using the Capco shaker for 10 minutes (Figure 2).

Figure 1: (left) Sieve selection
Figure 2: (right) Sieves on the shaker

No sand grading was supplied by the manufacturer so the results could not be compared but the particle size distribution is shown in Table 1.

Table 1: Particle size distribution of sea sand

Sieve size (mm)	2	1	0.5	0.4	0.315	0.250	0.125	0.063
Cumulative retained (%)	0.06	0.26	7.89	31.22	68.59	87.79	99.92	99.96

A graphical representation of the particle size distribution is shown in Figure 3.

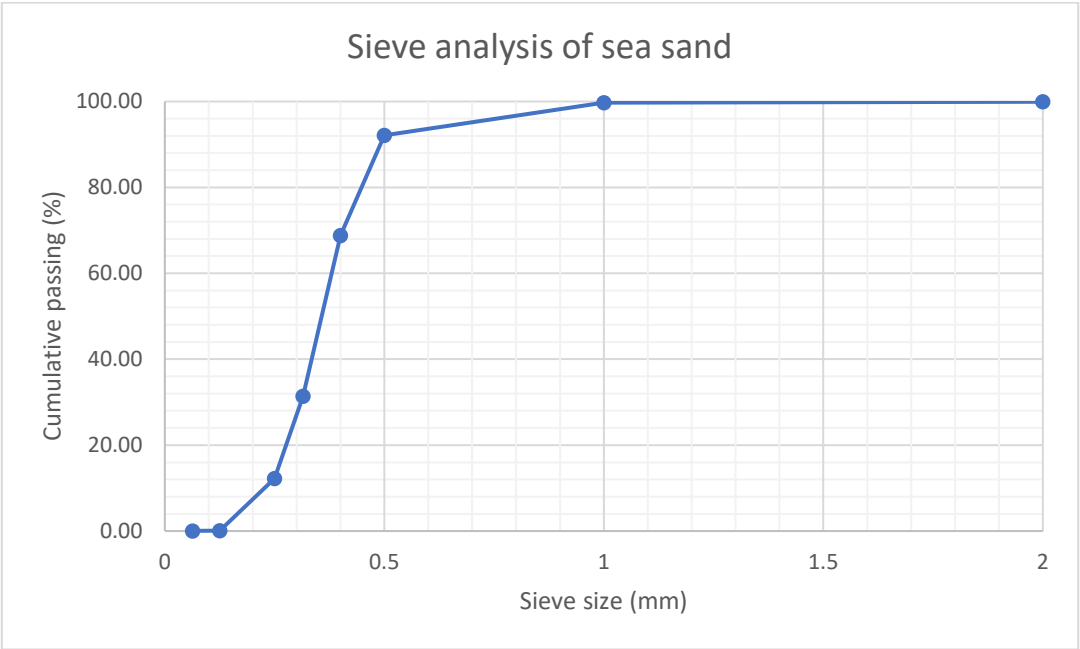

Figure 3: Particle size distribution

Water

The fresh water described was taken from the tap in BRL014 and was potable. Seawater was collected from the University Marine Station and had been passed through a UV steriliser and filtered for solids. Typical salinity is 33g of salt per kg.

Admixture

Rockbond Admix 201 powder is a water reducing admixture. This was used to reduce the water to cement ratio. 1% of admixture by weight of cement was added as recommended by the manufacturer's instructions. The specification and safety data sheet can be seen in Appendix C.

Sample Trials

Before the main concrete specimens were produced, various samples were made to determine a suitable mix and determine any problems. These were produced in BRL014 with the help of the lab technicians. Mixing was done in a bucket due to the small quantities as seen in Figure 4 and 5. Initial samples were based on a mix used by Ji (2018). The mix quantities can be seen in Table 2. Samples were tested at 3 days and showed there wasn't any noticeable difference in compressive strength when sea water was used in place of fresh water. One problem discovered was the presence of bubbles in mixes containing water reducer admixture.

Figure 4: Bucket mix

Figure 5: Trial mix cubes

However, the quantity of admixture used was higher than the manufacturer's instructions. It was also apparent the sample mixes containing admixture weren't as quick setting as expected and it wasn't possible to unmould the cubes after 24 hours unlike the samples which didn't contain admixture.

Table 2: Previously used mix ratio

w/b	Mortar mix ratio (kg/m^3)			
	Cement	Sea sand	Water	Water reducer
0.3	700	1400	210	20

The second set of samples were adjusted to contain 1% admixture as recommended by the manufacturer and were able to be unmoulded after 24 hours. There were also much less bubbles indicating the greater quantity of admixture was responsible for the bubbles and the increase in set time. The results can be seen in Table 3. An increase in w/b (water to binder) ratio from 0.3 to 0.4 showed workability improved slightly but reduced strength significantly. Admixture significantly improved strength despite w/b ratio staying at 0.3. The tests also showed sea water increased the strength of the concrete over fresh water.

Table 3: Trial results

Composition	w/b	Weight (kg)		Total load (kN)	Compressive strength (N/mm^2)
		Dry	Wet		
SS/SW/-	0.3	2.196	1.233	342	34.2
		2.191	1.236	341	34.1
SS/FW/AM	0.3	2.239	1.239	473	47.3
		2.237	1.236	471	47.1
SS/SW/AM	0.3	2.280	1.276	499	49.9
		2.237	1.252	508	50.8
SS/FW/-	0.4	2.174	1.193	252	25.2
		2.175	1.197	258	25.8

Mix quantities

The mix recipe will contain 1% admixture by weight of cement and a w/b ratio of 0.3 as can be seen in Table 4.

Table 4: Concrete mix

w/b	Mortar mix ratio (kg/m^3)			
	Cement	Sea sand	Sea/fresh water	Water reducer
0.3	700	1400	210	7

As previously mentioned, the marine dredged sand had likely been washed prior to use and so contained very little salt. Ideally the two mixes compared in the tests would be one including sea water and unwashed sea sand, and fresh water with washed sand. However, the only sand available in the lab is the washed sand. Therefore, the

options would be to soak the sand in sea water and drain it to replicate unwashed sea sand or add the extra salt that would have been left behind by the sea water.

As this extra quantity of salt or chlorides would be small in comparison with the quantity already in the sea water and unlikely to have any additional affect, it was decided to use the same sea sand as it was in both mixes. Therefore, the only variable between mixes is the water type, fresh water and sea water.

Beam Design

CFRP mesh

CFRP mesh used for the reinforcing was produced from 48k carbon and mesh gap sizing was 10mmx8.5mm. Breaking strength of the mesh was 1700N/mm^2 according to the data sheet seen in Appendix D. This was chosen due to having already been ordered by the university and was available for use.

From the specification (Appendix D) it can be calculated that the cross-sectional area of each tow should be 1.808mm^2. As seen in Figure 12, 6 lengths of tows would fit in the beam width. This is a total of 10.848mm^2 of CFRP. Theoretically this quantity of CFRP reinforcement would have a tensile strength of 18.44kN.

Further investigation in to the CFRP showed that the actual cross-sectional area was on average 3.236mm^2. This was taken by cutting the CFRP tows and using an Olympus BX60M microscope (Figure 6) to view and measure the cross-sectional area of each tow (Figure 7). 9 samples were used giving consistent results as confirmed by a CV (Coefficient of Variation) value of 3.35%. Cross sectional areas of the measured samples can be seen in Figure 8.

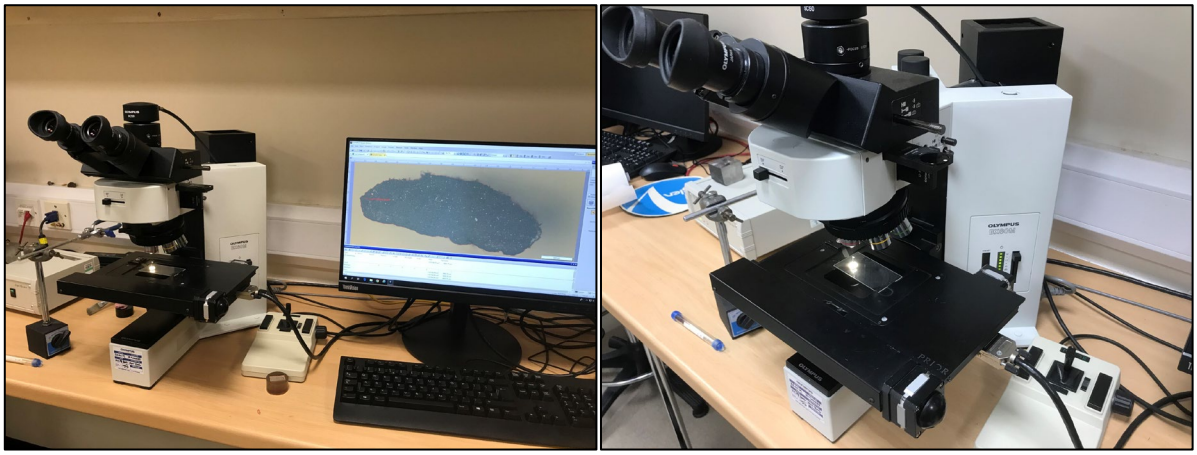

Figure 6: Measuring the cross-sectional area of CFRP tows

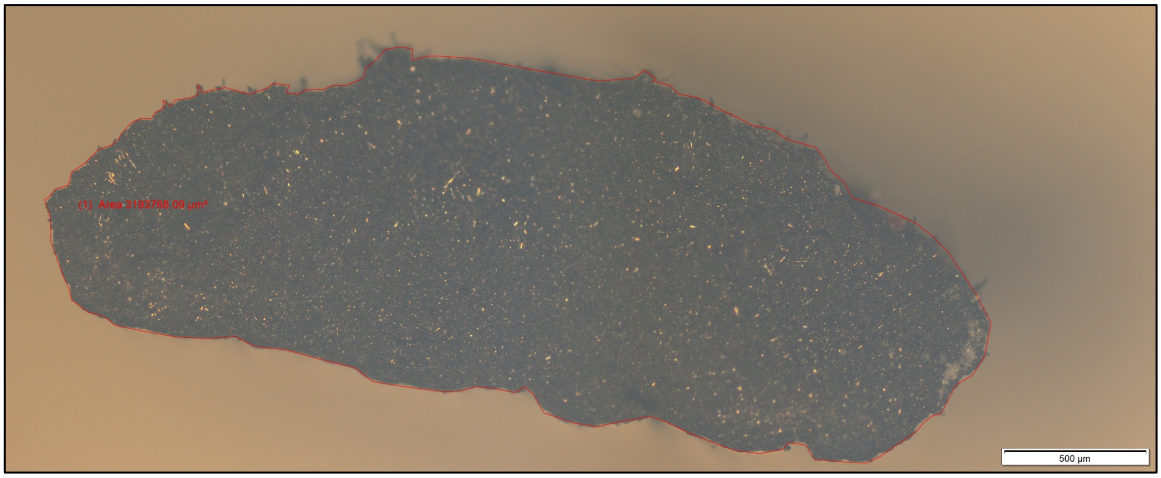

Figure 7: Microscopic image of CFRP tow

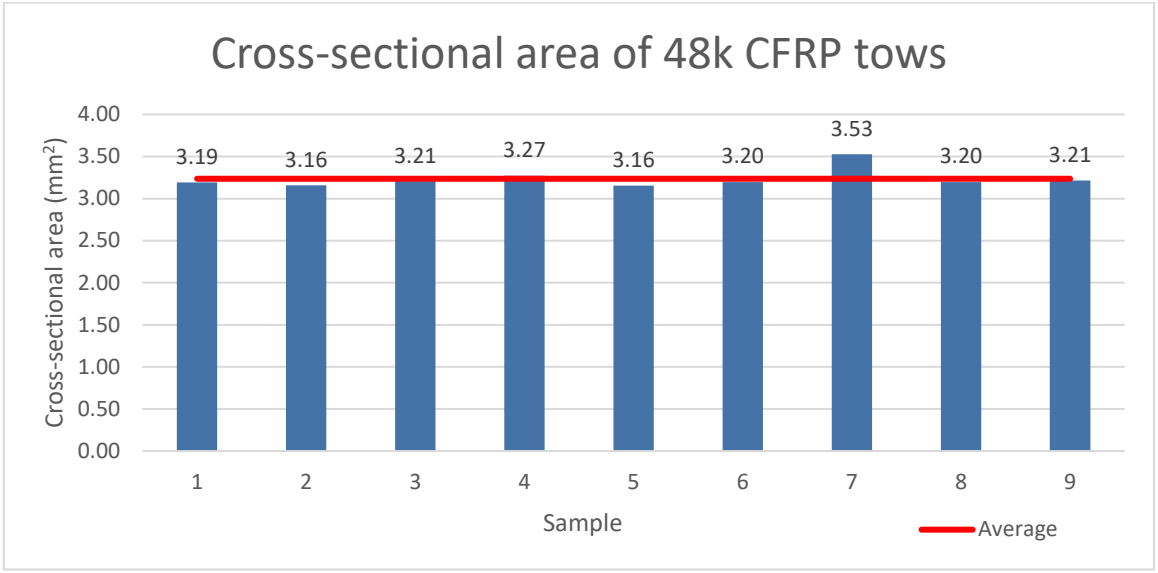

Figure 8: Cross-sectional areas of 48k CFRP tows

The findings indicated that the specification gives the net area of carbon fibre, excluding the epoxy used in the tows. Hence, the V_f (volume fraction ratio) of the CFRP based on this is 56%. It would be important to know which figure is given when calculating beam reinforcement. Knowing the V_f would be necessary if it was not the net area that is provided. Without this, the reinforcement may be severely under designed as the strength of the resin is much lower than carbon fibre.

Additionally, the Young's modulus of the carbon fibre was calculated from a tensile test performed on an individual tow. The specified cross-sectional area was used for this. The force vs displacement graph from the test can be seen in Figure 9. The area highlighted in red has been taken which is before the tow started to slip in the test rig. From this, the stress and strain values were calculated and plotted in Figure 10. The Youngs modulus of the carbon fibre can be taken as the gradient. It was found that the Young's modulus was 168GPa. This was lower than expected compared with

figures given between 200 and 960GPa by Bajpai (2013). However, this fits in to the given estimates of 165 to 215GPa by Adhikarinayake et al. (n.d). The test was only performed once however so more tests would be needed to confirm reliability. It may also have been possible that the tow was sliding through the grips at the end rather than elongating. This was because the grips could not be tightened too much without causing damage to the fibres which would concentrate stresses leading to failure.

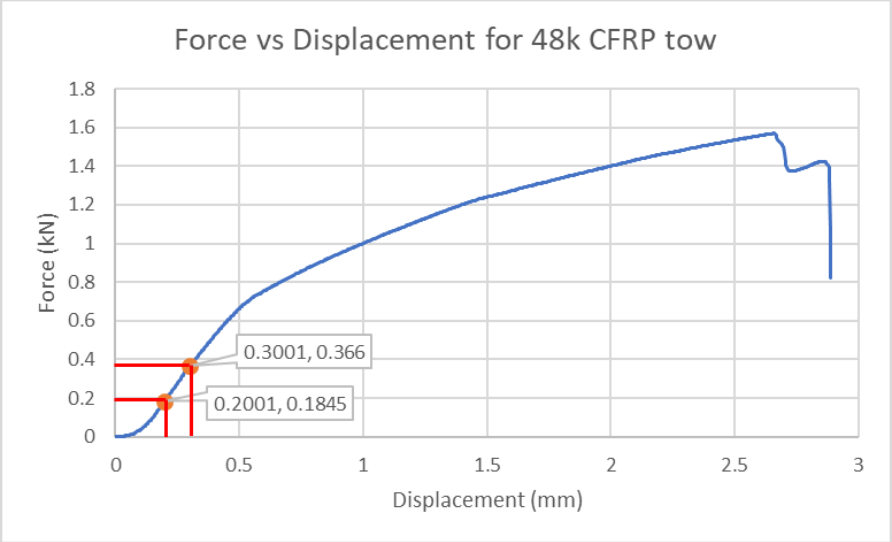

Figure 9: Force vs displacement of 48k CFRP tow during tensile test

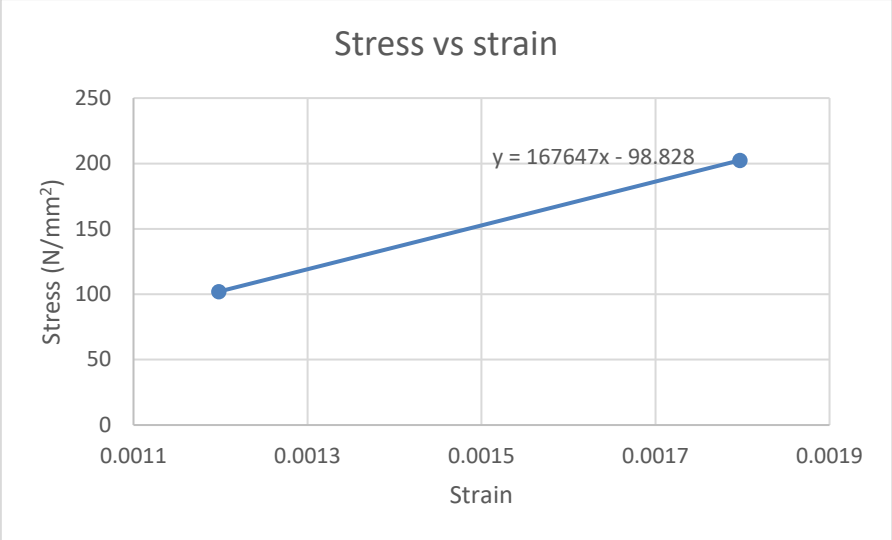

Figure 10: Stress vs strain graph

Design

The beam mould sizes were 100x100x500mm but inserts to hold the mesh were created from 10mm plastic which reduced the beam size to 80x100x480mm (Figure 11 and 22). Reinforcement mesh was placed 10mm from the bottom of the beam.

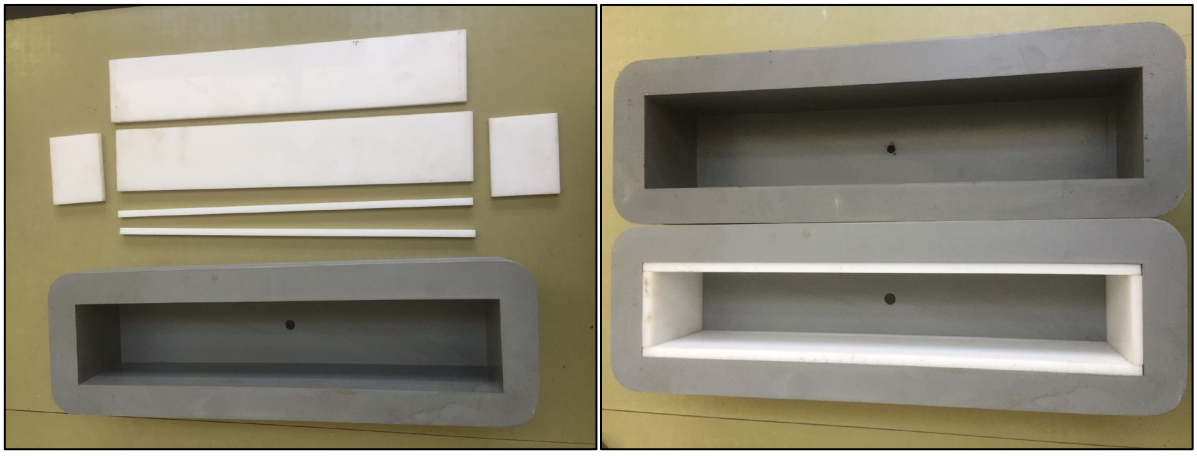

Figure 11: Mould and inserts

Casting

The number of samples produced can be seen in Table 5.

Table 5: Samples produced

Mix	Composition	Sample Type	Dimensions (mm)	Amount
1	SS/FW	Cubes	100x100x100	12
		Cylinders	Ø100x200	12
		Beams	80x100x480	4
2	SS/SW	Cubes	100x100x100	12
		Cylinders	Ø100x200	12
		Beams	80x100x480	4

SS = Sea sand FW = Fresh water SW = Sea water

Preparation & Casting

Due to the limited number of moulds available to use, the mixing dates of both mixes had to be staggered. Therefore FW (mix 2) was produced exactly one week after SW (mix 1). In preparation for mixing and casting, all moulds were cleaned and coated with releasing agent (Figure 13). CFRP mesh to be used as beam reinforcement was cut to size and put in place as seen in Figure 12. Additionally, a piece of tape was placed in the bottom of the mould to prevent the plug hole filling with concrete and the rubber plug inserted from the bottom side.

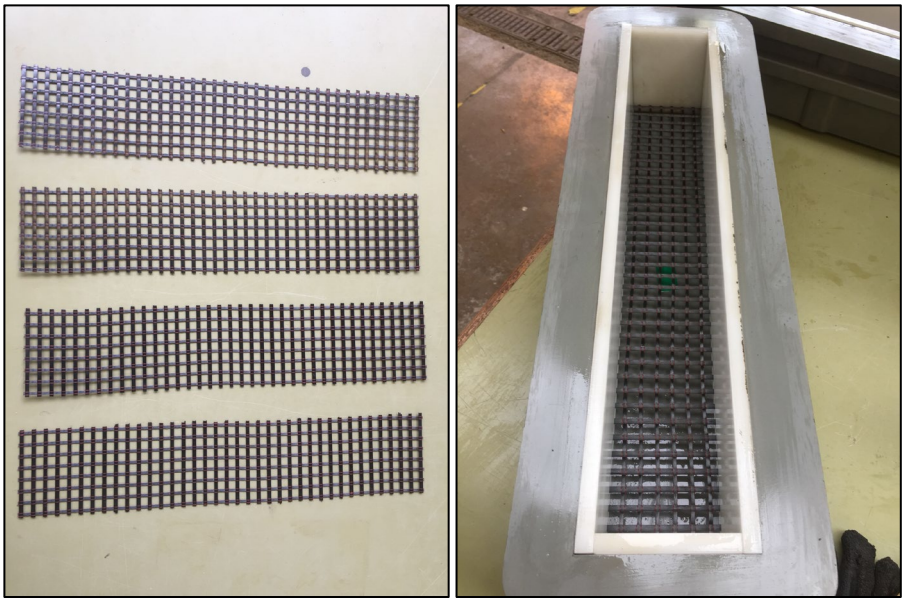

Figure 12: CFRP mesh cut (left) and put in mould (right)

The sand had been oven dried overnight and given enough time to cool before casting to avoid accelerating the setting time of the concrete (Figure 14).

Figure 13: (left) - Samples prepared and ready for mix
Figure 14: (right) - Sand being oven dried

All components of the concrete mix were weighed out using weighing scales. The admixture was mixed in with the water using a drill and mixing attachment. The cement mixer drum was wiped with a damp cloth prior to use to coat the surface and prevent absorption of the mix water. Half of the sand was added, then the cement and then the remainder of the sand was added on top of this to prevent the cement becoming airborne when mixed. Water was added to the mix and slightly worked in with a trowel before using the cement mixer for two minutes. The trowel was used to loosen any unmixed components on the edge of the drum then mixed for a further minute (Figure 15).

Figure 15: Concrete being mixed

Concrete was placed into the moulds and compacted using tamping rods and then the shaker table for the cubes and cylinders. The beams were compacted by lifting the edges of the mould and letting them fall on to the table whilst holding the inserts in place. This was due to the inserts used to hold the mesh in place not being secured and using the shaker table may have dislodged them. All samples were covered with plastic sheets to prevent excess water loss through evaporation until they were unmoulded.

Unmoulding

All samples were unmoulded 24 hours later and placed into a curing tank which contained fresh water at a constant 20°C until being tested (Figure 16 and 17).

Figure 16: (left) - Samples after unmoulding
Figure 17: (right) - Samples placed in curing tank

Testing

All testing of samples was carried out following the procedures noted in the relevant parts of BS EN 12390. All beams were tested at age 28 days whilst 12 cubes and 12 cylinders were produced with 4 of each tested at 7, 14 and 28 days. The testing procedure for both mixes was the same except that FW (mix 2) testing was carried out

one week after SW (mix 1) with many test dates overlapping. For example, 14-day testing for SW (mix 1) coincided with 7-day testing for FW (mix 2).

Densities

Cube and cylinder samples were weighed dry and in water before testing to determine the density (Figure 18 and 19). The beams could only be weighed dry as they would not fit in to the weighing tank.

Figure 18: (left) - Sample being weighed dry
Figure 19: (right) - Sample being weighed in water

Compressive Test

For compressive tests the procedure for testing was in accordance with BS EN 12390-3:2009 (British Standards Institution, 2009a). Samples were wiped surface dry and placed in to the TONIPACT 3000 hydraulic press. The machine load was balanced, and the cubes were loaded at a rate of 4.0kN/s until failure. The setup can be seen in Figure 20 and 21.

Figure 20: (left) - TONIPACT 3000 hydraulic press
Figure 21: (right) - Compressive test on cube

Tensile test

Cylinders were also tested using the TONIPACT 3000. Testing was carried out in accordance with BS EN 12390-6:2000 (British Standards Institution, 2000). As seen in Figure 22 the cylinders were loaded into the testing jig with packing strips top and bottom between the metal plates before the machine was loaded at 1.5kN/s until failure (Figure 23).

Figure 22: (left) - Tensile test on a cylinder
Figure 23: (right) - Broken cylinders after testing

Flexural test

Flexural testing was carried out using the Instron machine in Smeaton lab (Figure 24). A four-point flexural test was carried out on the beams for reasons mentioned previously in Section 2.8. Testing was carried out in accordance with BS EN 12390-5:2009 (British Standards Institution, 2009b) therefore the lower supports were spaced at 300mm and the loading rollers at 100mm. The position of rollers and supports can be seen in Figure 25. The beam was preloaded with 100N and it was decided the beam would be loaded at a rate of 0.5mm/minute. Displacement loading rather than force loading was chosen as it was thought this would provide a more controlled test.

Figure 24: (left) - Instron machine used for flexural test
Figure 25: (right) - Beam undergoing flexural test

Results

Density results

The average density for SW and FW mixes based on cube and cylinder results are shown in Table 6. The individual densities for each sample can be seen in Appendix E. As the beams could not be weighed in water it was not possible to determine their density. As the beams were from the same mix as their respective cubes and cylinders it could be assumed they have the same density as shown in Table 6.

Table 6: Average density of each mix based on cubes and cylinders

	Density (kg/m^3)
Mix 1 (SW)	2224
Mix 2 (FW)	2184

Compressive strength results

The maximum loads reached for cube samples in the compressive test can be seen in Table 7. Full results for the cube samples can be seen in Appendix E.

Table 7: Maximum loads reached in compressive test for SW and FW cubes

Mix 1 (SW) Compressive test		
Cube	Age	Maximum load (kN)
1	7 days	592
2		588
3		582
4		593
5	14 days	607
6		582
7		623
8		603
9	28 days	683
10		642
11		682
12		681

Mix 2 (FW) Compressive test		
Cube	Age	Maximum load (kN)
1	7 days	512
2		535
3		517
4		508
5	14 days	613
6		604
7		562
8		550
9	28 days	641
10		617
11		598
12		648

Tensile strength results

The maximum loads reached for cylinder samples in the tensile test can be seen in Table 8. Full results for the cylinder samples can be seen in Appendix E.

Table 8: Maximum loads reached in tensile test for SW and FW cylinders

Mix 1 (SW) Tensile test		
Cylinder	Age	Maximum load (kN)
1	7 days	147.7
2		147.4
3		141.7
4		127.9
5	14 days	145.6
6		144.8
7		133.6
8		148.9
9	28 days	180.1
10		147.3
11		151.2
12		147.5

Mix 2 (FW) Tensile test		
Cylinder	Age	Maximum load (kN)
1	7 days	135.6
2		144.2
3		125.7
4		134.5
5	14 days	129.9
6		138.1
7		141.5
8		145.3
9	28 days	148.1
10		146.1
11		142.5
12		150.8

Flexural strength results

The results of the 28-day flexural test for SW can be seen in Figure 26.

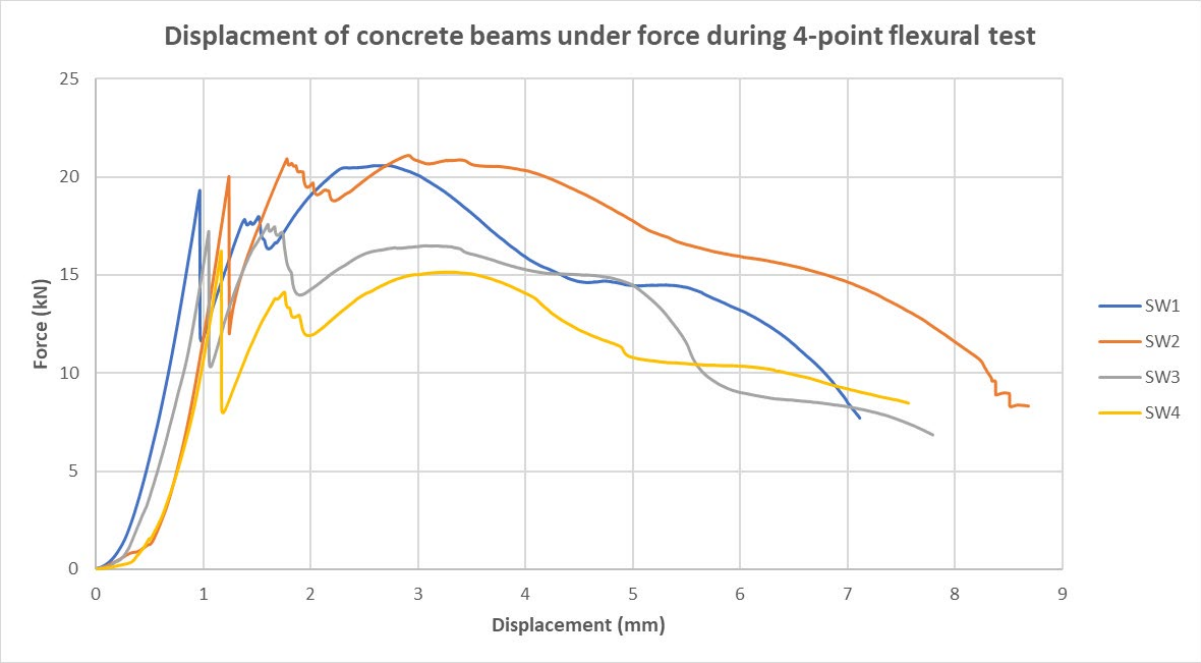

Figure 26: SW concrete at 28 days flexural results

The results of the 28-day flexural test for FW can be seen in Figure 27. FW1 only displays results until 3mm displacement due to a user error after this point. Data up until 3mm is correct and the same procedure was carried out as the other beams.

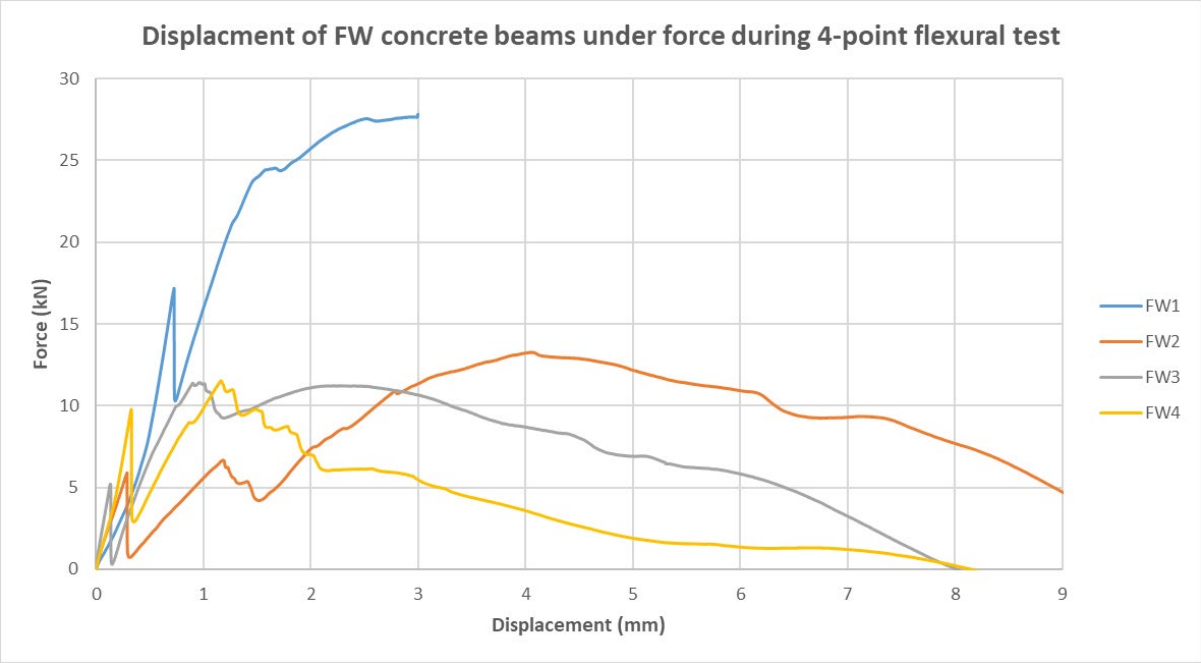

Figure 27: FW concrete at 28 days flexural results

Calculations

Density calculations
Density is calculated from

$$D = \frac{m}{V}$$

$$V = \frac{m_a - m_w}{p_w}$$

$$D = \frac{m}{(\frac{m_a - m_w}{p_w})}$$

V = volume (m^3)
m_a = mass of specimen in air (kg)
m_w = mass of specimen in water (kg)
p_w = density of water (kg/m^3)
D = density (kg/m^3)

Compressive strength calculations
The compressive strength is calculated from

$$f_c = \frac{F}{A_c}$$

f_c = compressive strength (N/mm^2)
F = maximum load (N)
A_c = cross sectional area of cube (mm^2)

Tensile strength calculations
The tensile strength is calculated from

$$f_{ct} = \frac{2 * F}{\pi * L * d}$$

f_{ct} = tensile splitting strength (N/mm^2)
F = maximum load (N)
L = length of line of contact (mm)
d = cross sectional dimension (mm)

Flexural strength calculations
The flexural strength is calculated from

$$f_{cf} = \frac{F * I}{d_1 * {d_2}^2}$$

f_{cf} = flexural strength (N/mm^2)
F = maximum load (N)
I = distance between supporting rollers (mm)
d_1 and d_2 = lateral dimensions of beam (mm)
The maximum loading force for unreinforced beams is calculated from

$$M_{max} = \frac{\sigma_{max} * I}{y * {L}/{3}}$$

$$F_{max} = \frac{M_{max}}{{L}/{3}}$$

M_{max} = maximum bending moment (Nmm)
σ_{max} = maximum tensile stress (based on 28-day cylinder tests) (N/mm^2)
I = second moment of area of beam (mm^4)
y = distance from neutral axis to edge of beam (mm)
L = distance between supporting rollers (mm)
F_{max} = maximum force (N)

Discussion

Density of specimens

As seen in Table 6 the average density of the SW samples was 2224kg/m^3 while the FW density was 2184kg/m^3. This is a difference of 40kg/m^3. When casting the concrete samples, it became evident that bubbles were present in both mixes. Some possibly one-off occurrences of poor compaction (Figure 28) whilst the rest were entrained air throughout (Figure 29).

Figure 28: (left) - Bubbles possibly a result of poor compaction
Figure 29: (right) - Entrained air throughout samples

This was despite the specification (Appendix C) stating that the admixture "Will not entrain air". It was thought that the entrained air bubbles were in fact due to the addition of the admixture because sample mixes without admixture had only very small bubbles. The difference in quantity and size of bubbles can be seen from Figure 30 and 31. This confirms the bubbles are not due to the sea water or sea sand but caused by the admixture.

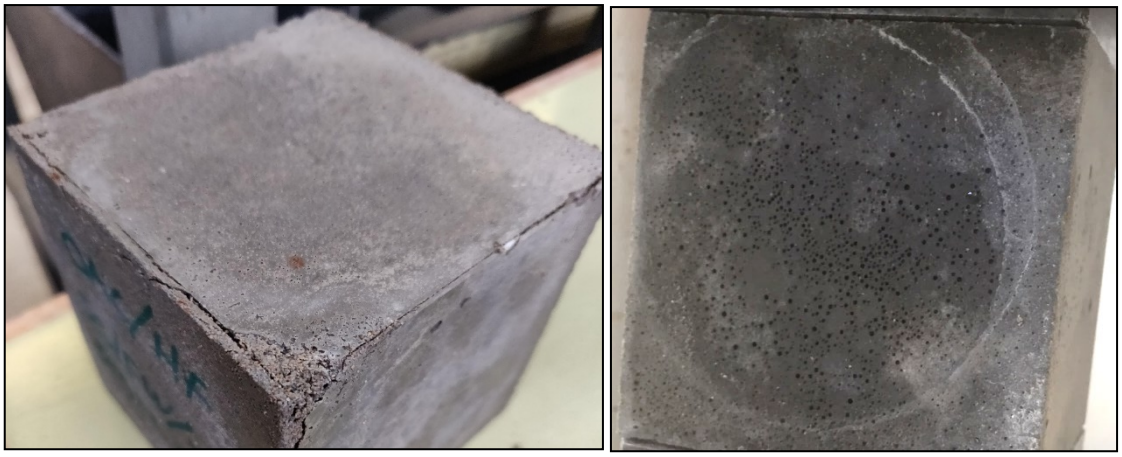

Figure 30: (left) - Without use of admixture
Figure 31: (right) - Addition of admixture

On closer inspection of samples after testing, it became clear that the SW batch was better mixed than the FW. The insides of tested SW cylinders can be seen in Figure 32 and FW in Figure 33. The SW is evenly mixed, whereas the FW appears to have many unmixed clumps of cement. This was initially noticed when mixing the ingredients together. The cement had been emptied from its bag and clumps had started to form possibly due to moisture or the cement starting to go off. The cement

was still in date however so this should not have been a problem. Usually during the mixing stage clumps like this would break up with larger aggregates but as this mix only included fine aggregates this did not happen.

Therefore, one possible reason for the lower density of FW mix could have been due to the lack of distribution of cement throughout. Additionally, as the difference is very small, this could have been due to errors in weighing, perhaps the samples were not fully surface dry when being dry weighed, or the scales were not accurate. Or this error may have occurred from variations in sample sizes which could also affect the results.

Figure 32: (left) - SW cylinders after testing
Figure 33: (right) - FW cylinders after testing

Compressive strength

The compressive strength of SW samples can be seen in Figure 34. The strength values for all age samples are reliable as confirmed by their CV, 0.73, 2.42 and 2.58%. With one exception, the compressive strength has continually increased with age. The only instance where it has not is at 14 days, where a cube of 58.2N/mm^2 was recorded. This was the same as the lowest value from 7 days. The strength was expected to increase as time progressed, although the average increase in strength from 7 days to 14 days was only 1.5N/mm^2 which is very similar to the standard deviation so it would be likely for a value to lie outside this range anyway. The average gain from 14 to 28 days was 6.8N/mm^2 which still quite small indicated that most of the strength was gained very early on, within 7 days.

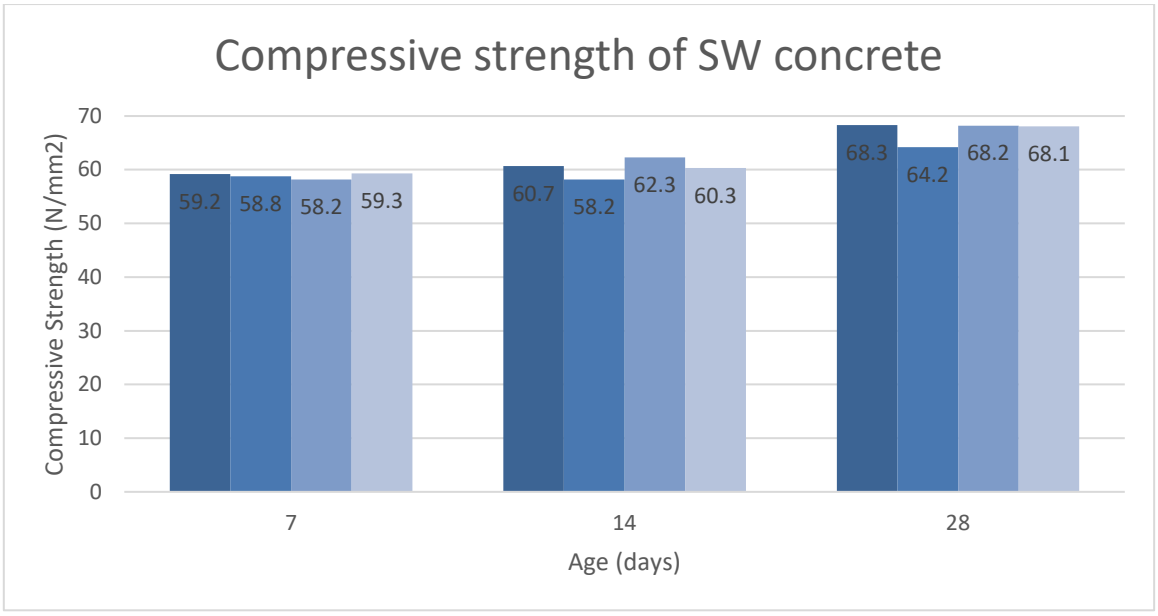

Figure 34: Compressive strength of SW concrete

Compressive strength of the FW concrete can be seen in Figure 35. The CV of the samples at each age is 1.99, 4.60 and 3.17%. This is a slightly bigger variation than with the SW samples, but the results are still reliable with no clear anomalies. Again, all except one sample have shown an increase in strength with age. The exception is at 28 days the lowest strength value was 59.8N/mm^2 which was lower than two of the 14-day samples, although this is still higher than the average 14-day value.

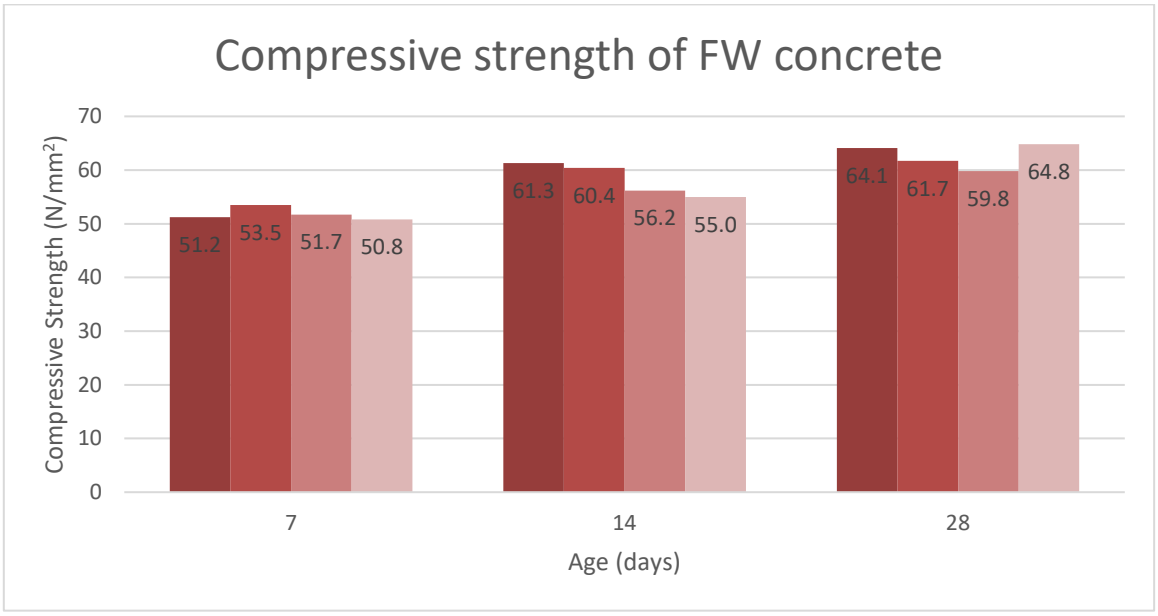

Figure 35: Compressive strength of FW concrete

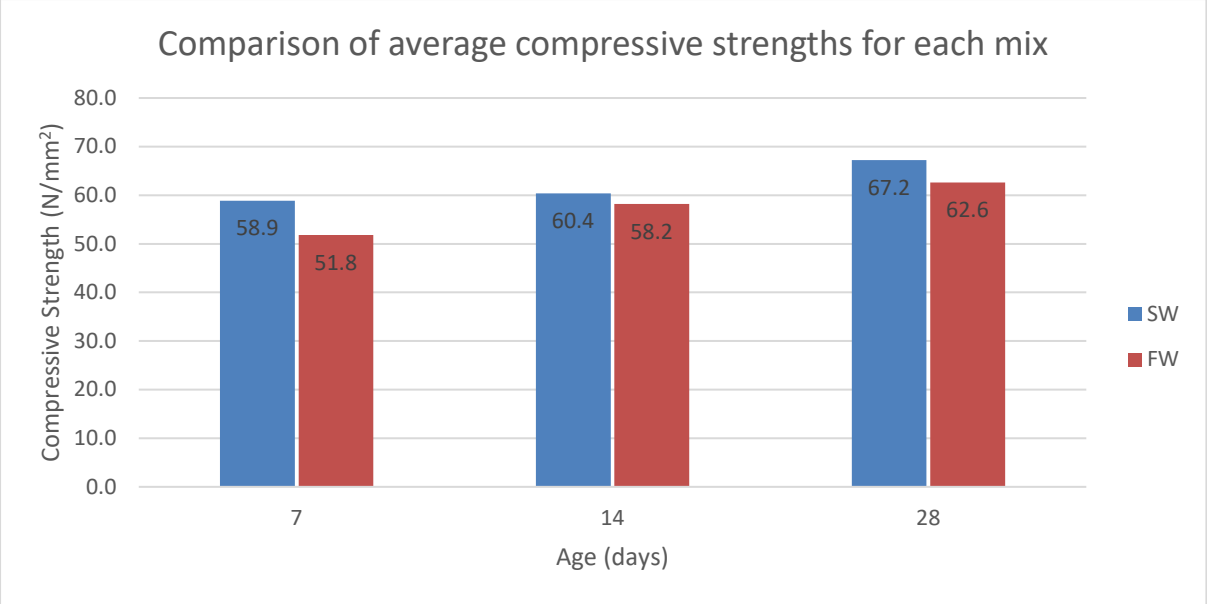

Figure 36: Comparison of SW and FW compressive strengths

As seen in Figure 36, for SW 87.6% of its 28-day strength was gained within the first 7 days and 89.9% at 14 days. For FW this value was 82.7% at 7 days and 92.9% at 14 days. This indicates that SW had better early strength gain at 7 days, however FW had better early strength gain at 14 days. This however does not mean FW was stronger at 14 days.

SW strength was more than FW at all ages. In comparison with FW, the SW had a higher strength of 13.7%, 3.8% and 7.3% at 7, 14 and 28 days respectively. The testing carried out cannot explain why SW has caused an increase compared with using FW.

The concretes can be graded as 64MPa for SW and 59MPa for FW based on their characteristic compressive strengths at 28 days. This is based on a normal distribution of the concrete samples where no more than 5% will fall below the given value.

It is also worth noting that as expected the samples show a positive correlation between density and compressive strength. Figure 37 shows this is a correlation with all sets of samples.

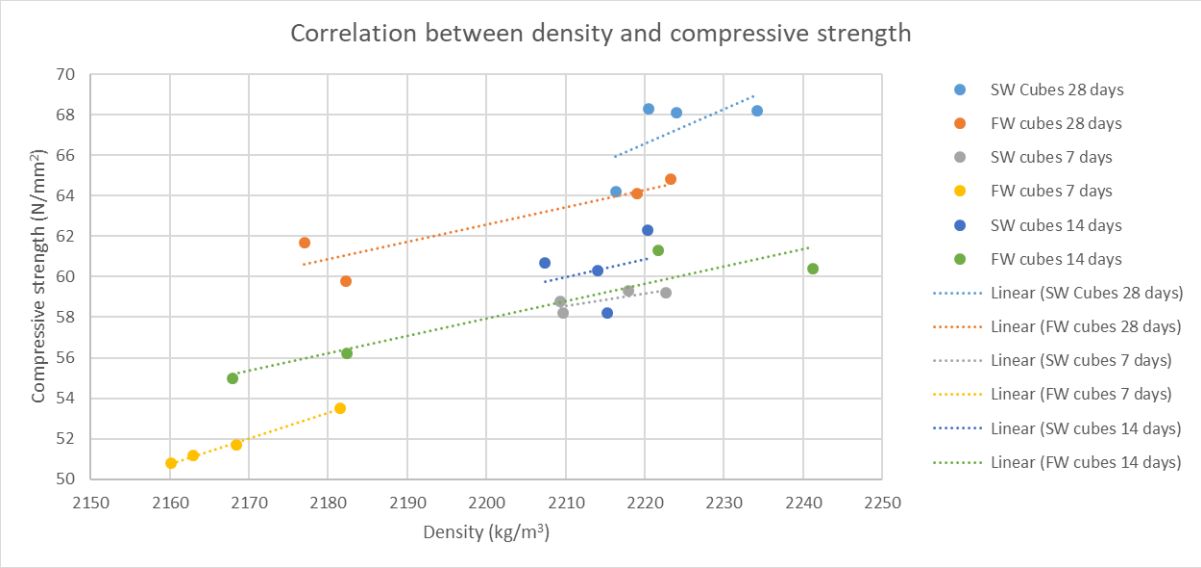

Figure 37: Correlation between density and compressive strength

Tensile strength

Tensile strengths for SW are shown in Figure 38 and it looks as if there is little change in tensile strength with age. CV for ages are 5.69, 4.03 and 8.75% so the data is reliable. However, the average strength for 28 days is 5N/mm^2 so the highest value of 5.73N/mm^2 lies outside of this variation.

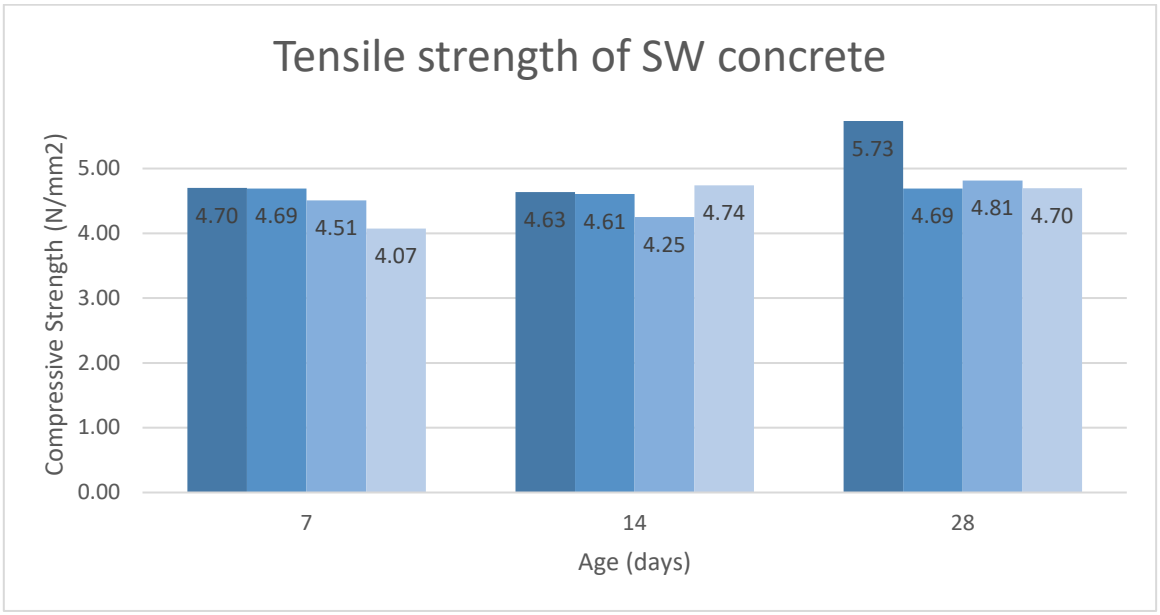

Figure 38: Tensile strength of SW concrete

The tensile strengths for FW are shown in Figure 39. Again, there is little change in the strength with age and the values also look reliable. This is confirmed with CV of 4.85, 4.10 and 2.06%. This is slightly better than with the SW values, however both are consistent.

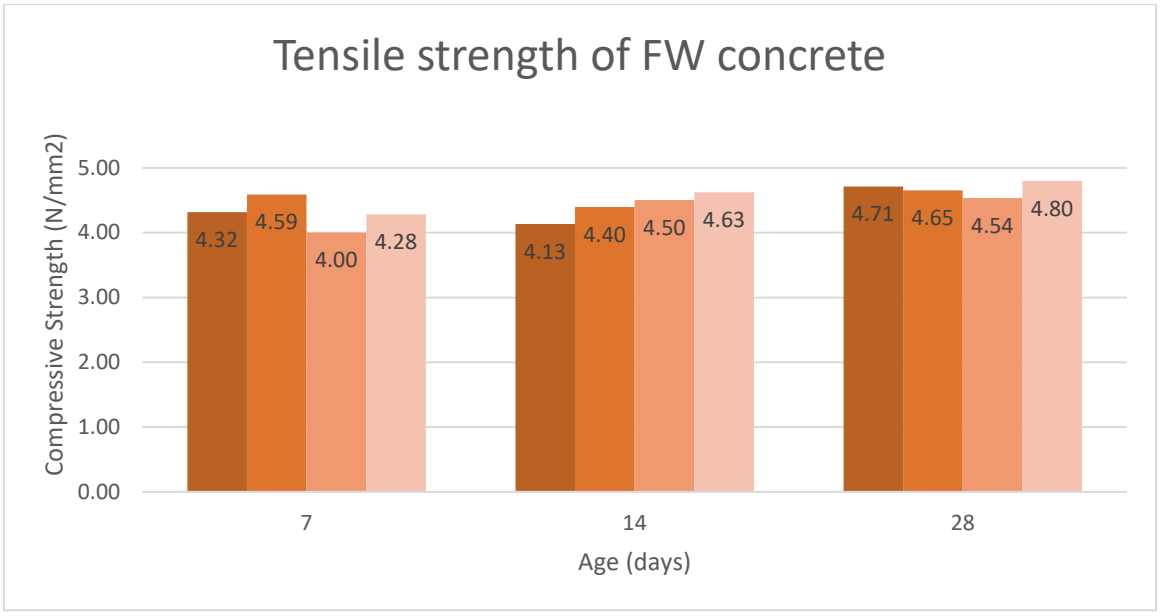

Figure 39: Tensile strengths of FW concrete

The average tensile strengths of both SW and FW are compared in Figure 40. This shows that for both mixes, tensile strengths have increased with age though only very slightly. The biggest gain for both was between 14 and 28 days as opposed to 7 and 14 days. It also shows that SW had a higher tensile strength at all ages compared with FW. SW and FW gained 90% and 91.5% of their 28-day strengths by 7 days. At 28 days SW had a 6.4% greater strength than FW.

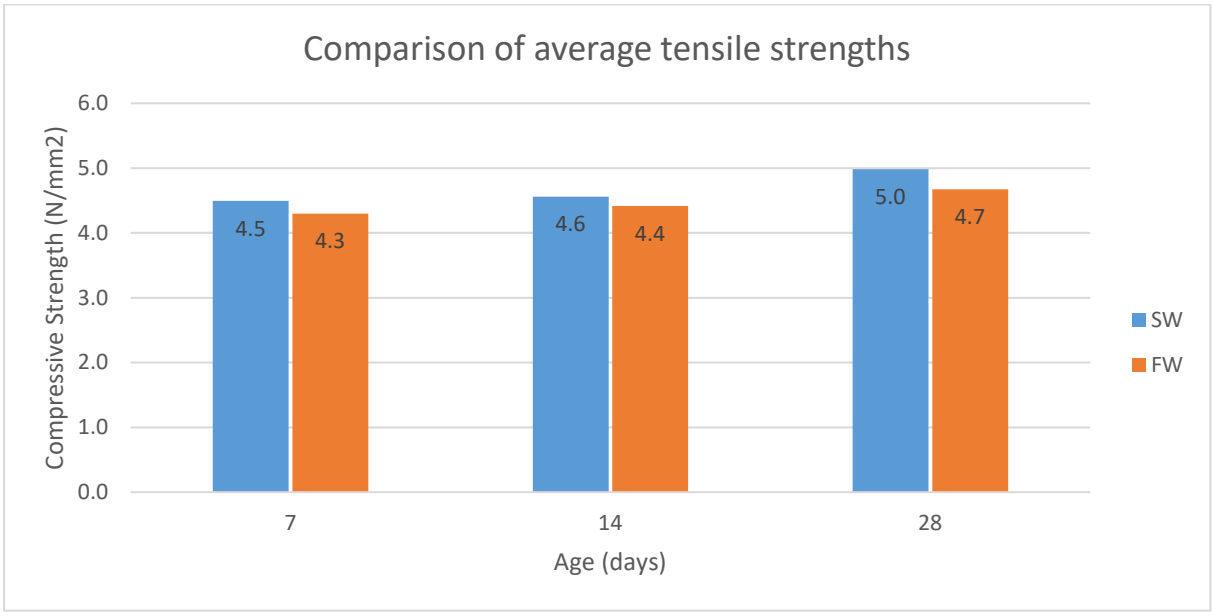

Figure 40: Comparison of tensile strengths for SW and FW concrete

As previously mentioned, it is expected a higher density would correlate with higher strength. As can be seen from Figure 41, most sets of cylinder samples do not follow this trend. However, each set only contained 4 samples and a larger quantity would be needed to give a more reliable distribution.

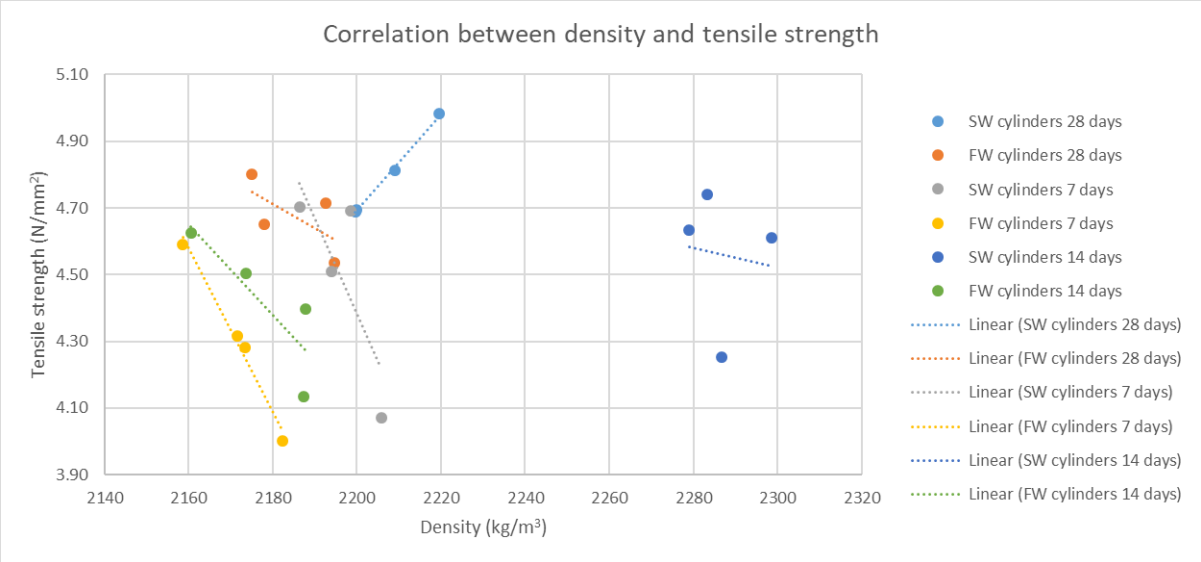

Figure 41: Correlation between density and tensile strength

Flexural strength

From the 4-point flexural bending test the maximum loads for each beam can be seen in Table 9. On average SW appears to have a much higher maximum load.

Table 9: Maximum loads of beams undergoing flexural test

Mix 1 SW	
Beam	Maximum load (kN)
1	20.58
2	21.10
3	17.58
4	16.22

Mix 2 FW	
Beam	Maximum load (kN)
1	27.83
2	13.27
3	11.42
4	11.52

The average maximum load for SW was 18.9kN and for FW it was 16.0kN. This would suggest SW had a better flexural strength. Despite the highest maximum load being from a FW beam the CV for SW is 10.79% and for FW it is 42.87% suggesting the data for SW is much more reliable. It is possible the FW values are less accurate as seen by the variation of results.

Appendix F shows the beams after failure from the flexural test. All beams have failed in bending as seen from vertical fractures developing in the bottom of the beams. It was expected that beams would fail in between the loading rollers as this is where the

bending moment would be greatest. All beams appear to have failed off-centre within this range. Failure appears to have occurred in the same manner with a vertical or diagonal fracture propagating up through roughly 90% of the beam before deviating diagonally towards the centre of the beam.

The highest maximum load recorded was for FW. This value is over double the other FW values. When looking at Figure 26 and 27 it appears that FW1 is an anomaly as it isn't consistent with the other FW beam results. However, the SW and FW results weren't expected to differ much and as FW1 is similar to the results for SW it makes it seem more like FW2, FW3 and FW4 are inconsistent.

Table 10: Theoretical maximum breaking force for unreinforced beams

	SW	FW
I (mm^4)	6666667	6666667
y (mm)	50	50
σ_{max} (N/mm^2)	4.98	4.68
L (mm)	300	300
M_{max} (Nmm^2)	664313	623357
F_{max} (kN)	13.3	12.5

Table 10 shows the theoretical maximum loads for unreinforced beams subject to the flexural test. The addition of reinforcement would be expected to increase the maximum load. This is in line with the maximum loads for SW shown in Table 9 as they are higher than the unreinforced values. However, with FW only two of the beams reached a higher load than unreinforced beams were expected to reach. When comparing the average maximum load for reinforced beams (Table 9) and theoretical unreinforced beam maximum load (Table 10) the addition of CFRP has improved flexural strength by 42.1% in SW and 28% for FW.

Table 11: Flexural strength of beams

Mix 1 SW	
Beam	Flexural Strength (N/mm^2)
1	7.7
2	7.9
3	6.6
4	6.1
Average	7.1

Mix 2 FW	
Beam	Flexural Strength (N/mm^2)
1	10.4
2	5.0
3	4.3
4	4.3
Average	6.0

Furthermore, the flexural strengths of the beams are shown in Table 11. SW beams on average had a higher flexural strength. This was 7.1N/mm^2 compared to 6.0N/mm^2 for FW, an 18.3% greater flexural strength. A reason for this large increase in flexural strength is unknown. One possibility is the chlorides which also lead to an increase in

strength have caused better bonding between the concrete and the CFRP. Or that somehow the chlorides had enabled the concrete to allow more flex before cracking. It is also possible that reduced strength in the FW beams were due to problems in the testing process. As the top face of some beams were uneven from the casting, the beams may have been loaded unequally from the two rollers, although this can't be confirmed. It is important that more testing be carried out to confirm the findings as the results are varied and more testing will increase the reliability of this.

One of the major properties worth analysing is the interface between the CFRP and concrete. The two materials are designed to work in conjunction with each other and if this is not the case the full potential of the design will not be met. As the main aim of the CFRP is to withstand tensile forces, the concrete must be securely bonded with the CFRP as otherwise the concrete may fail before the CFRP under these forces. It is suspected this was the case with the beams tested.

On closer visual inspection of the CFRP within the beams after failure, it looked as if the bond between the CFRP and concrete were not working as planned and the CFRP was likely slipping inside the concrete.

The strain of the CFRP could be calculated from

$$\varepsilon = \frac{\sigma}{E} = \frac{1700MPa}{168\,000\,MPa} = 1\%$$

The length of the CFRP embedded in the beam was 480mm indicating 4.8mm of elongation would be expected. Therefore, it would be expected that the maximum width of the fracture in the beam would also be 4.8mm and as seen in Appendix F, the fractures were much wider. This again indicates that the width of the crack was not due to the elongation of the CFRP and likely that the bond between the CFRP and concrete had failed.

It is therefore clear that the adhesion between CFRP and concrete is insufficient. Better grip is needed between the two materials for the full potential of the CFRP to be met. With conventional steel reinforced concrete bond strength isn't usually a problem. Although rebar is usually ribbed to improve the bond strength. The CFRP doesn't have any ribs and is instead smooth so this may be one reason for the lack of bond strength. It may also have been beneficial to the bond strength for some shrinkage to occur to the concrete as Doria, Sales and Andrade (2015) suggests shrinkage would promote bond strength to steel rebar. According to Koratich (n.d.) the water content has the biggest influence on shrinkage and an increase in water content of 1% will increase shrinkage by 3%. As the concrete mix used included a water reducing admixture and had a low w/b ratio, the shrinkage may have been minimal. It may have been advantageous for the water ratio to have been increased, hence increasing shrinkage.

Doria, Sales and Andrade (2015) also state that epoxy resin coating to steel rebar reduces the concrete to steel bond strength. As the carbon fibre is also coated in epoxy, this may have had a similar affect. Another possible reason for the low bond strength could be the low reinforcement cover. Sonebi, Davidson and Cleland (2011) found that by increasing the concrete cover to steel rebar from 20mm to 50mm, bond

strength was improved by 30%. Cover to the CFRP in the concrete beams tested was just 10mm so increases in this may have increased bond strength.

Recommendations

As seen with the FW mix, cement clumps were present throughout the mix. This may or may not have impacted the results of the experiment. It is likely this would have reduced the performance of the FW concrete but by how much is not known. In future research it would be important to inspect the cement before use and sieve the cement if necessary, to remove clumps. This would ensure a true representation of the performance gain of SW over FW.

Additionally, the study covered testing of the concrete up to an age of 28 days. SW clearly had better performance during this period as shown from testing at 7, 14 and 28 days. It would however be interesting to see how the performance of the concrete develops in the long run thereafter this age.

During the flexural test of beams, in future it may be of benefit to either sand the top face of the beams smooth or to use a wooden packing plate to the top as done with the cylinder tensile testing. This would take up any abnormalities in the surface allowing the load to be evenly distributed between the two rollers.

The use of CFRP mesh was straight forward for use in the beams produced in this experiment, however on a larger scale, for example casting reinforced beams on site, it would be very difficult to manage the CFRP. This is because unlike steel, which is very ductile, the carbon fibre is much more susceptible to damage. Any impacts to the fibres can cause damage which would concentrate stresses to the damaged area likely weakening the reinforcement. This was shown when working with the CFRP and carrying out preliminary tensile tests on individual tows from the mesh. As seen in Figure 42 the CFRP tow failed where there were indents caused by the connection to the transverse tows in the mesh. The indents can be seen in Figure 43.

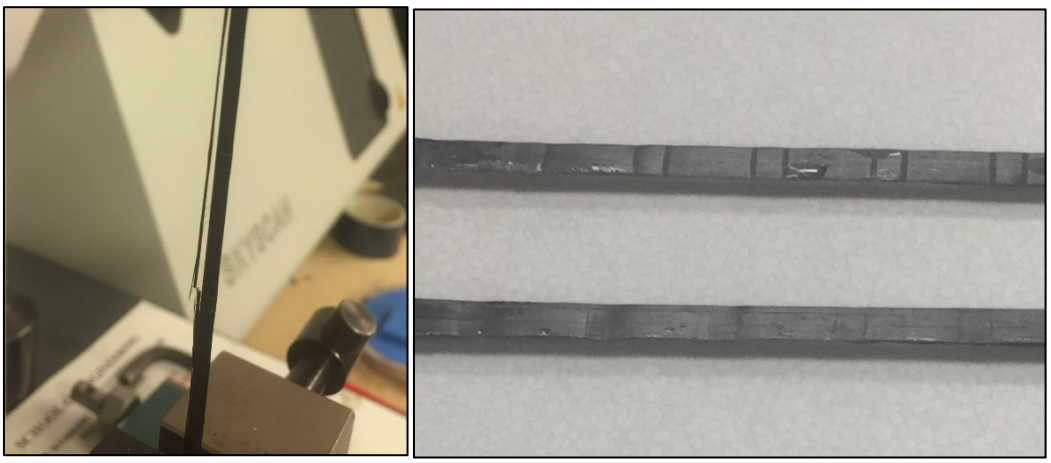

Figure 42: (left) - Failure in CFRP tow
Figure 43: (right) - Indents in CFRP from mesh connections

Small damage to the CFRP like this may occur from impacts which would otherwise leave steel unaffected. It is therefore recommended that this type of CFRP mesh would be better for use in precast elements where the CFRP could be used in a more controlled environment.

Additionally, as seen from the flexural testing, it was apparent that the interface between the CFRP and the concrete was not strong enough for the two materials to work together. Methods of improving the bond between them would be necessary to avoid slipping and prevent the failure of the bond before the failure of the CFRP under tension. Further research in this area would be beneficial for improved use. Pull out tests of CFRP within concrete, particularly a comparison of SW and FW concrete would be of interest to investigate if the difference in flexural results were a result of this or other causes. Moreover, whether if without the addition of admixture, the bond may have improved. It may have been possible that the bubbles induced by the admixture led to a reduction in bond strength. Also, as previously mentioned increasing the w/b ratio may increase shrinkage leading to improved bond strength. Additionally, further research into whether reinforcement cover affects bond strength of CFRP would be of interest.

Conclusions

Based on the findings of this research it can be concluded that SW has contributed a clear performance improvement over conventional FW concrete. The greatest improvement was regarding the compressive strength. SW increased the early strength gain at 7 and 14 days and by 28 days had a 7.3% higher strength than FW. Again at 7, 14 and 28 days SW concrete had a higher tensile strength than FW and at 28 days was 6.4% stronger. The flexural strength for SW concrete was thought to be 18.3% higher than FW based on the findings. Also, the addition of CFRP in the concrete beams was estimated to increase flexural strength over unreinforced beams by 42.1% in SW and 28% in FW. However, as there are inconsistencies with these results it is recommended further tests be carried out.

It was clear that the bond strength between the CFRP and the concrete was the main problem in the tests performed. Improvements in the bond strength would need to be investigated further and enhanced if possible to make the use of CFRP in concrete effective. Though, if CFRP were to be used as a reinforcement replacement for steel in concrete, then it could be very beneficial to use SW instead of FW for the performance gains covered in this paper. On top of this, using SW could reduce costs and environmental impacts compared with FW.

Acknowledgements

Throughout this research I have been given a great deal of assistance. Firstly, I would like to thank my supervisor Dr Shanshan Cheng for her guidance and the opportunity to carry out my research. Additionally, I would like to thank Trevor Bevan, Tony Tapp, Terry Richards, Richard Cullen, Jie Ji and Oliver Anderson-Chapman for their help and expertise during the laboratory processes.

References

Adhikarinayake, S., Gayan, K., Thathsarani, N. and Gamage, J. (n.d.). *Performance of Epoxy Adhesive Bond between CFRP and Concrete*. Undergraduate. University of Moratuwa.

Bajpai, P. (2013). *Update on carbon fibre*. Shrewsbury: Smithers Rapra Technology. Available at: https://app.knovel.com/hotlink/toc/id:kpUCF00002/update-carbon-fibre/update-carbon-fibre [Accessed 27/11/2018]

British Standards Institution. (2000). BS EN 12390-6:2000. 'Testing hardened concrete – Part 6: Tensile splitting strength of test specimens' Construction Information Service.

British Standards Institution. (2009a). BS EN 12390-3:2009. 'Testing hardened concrete – Part 3: Compressive strength of test specimens' Construction Information Service.

British Standards Institution. (2009b). BS EN 12390-5:2009. 'Testing hardened concrete – Part 5: Flexural strength of test specimens' Construction Information Service.

Doria, M., Sales, A. and Andrade, N. (2015). *Bond strength between stell-concrete and between concretes with different ages in structural rehabilitation*. [online] SciELO. Available at: http://www.scielo.br/scielo.php?script=sci_arttext&pid=S1983-41952015000500004#B12 [Accessed 30 Apr. 2019].

Gjorv, A B. (2009) Interviewed by Jorn Madslien for BBC News, 5 June. Available at: http://news.bbc.co.uk/1/hi/8085551.stm [Accessed 11 April 2019].

Ji, J. (2018) Conversation with Henry Farnell, 6 November.

Koratich, D. (n.d.). *Drying Shrinkage*. [online] Engr.psu.edu. Available at: https://www.engr.psu.edu/ce/courses/ce584/concrete/library/cracking/dryshrinkage/dryingshrinkage.html [Accessed 29 Apr. 2019].

Miller, S., Horvath, A. and Monteiro, P. (2018). Impacts of booming concrete production on water resources worldwide. *Nature Sustainability*, [online] 1(1), pp.69-76. Available at: https://www.nature.com/articles/s41893-017-0009-5#ref-CR27 [Accessed 13 Nov. 2018].

Ridoutt, B. and Pfister, S. (2010). A revised approach to water footprinting to make transparent the impacts of consumption and production on global freshwater scarcity. *Global Environmental Change*, [online] 20(1), pp.113-120. Available at: https://www.sciencedirect.com/science/article/pii/S0959378009000703#bib7 [Accessed 13 Nov. 2018].

Sonebi, M., Davidson, R. and Cleland, D. (2011). Bond between Reinforcement and Concrete – Influence of Steel Corrosion. *International Conference on Durability of Building Materials and Components*, [online] 10. Available at: https://www.researchgate.net/profile/M_Sonebi/publication/259656675_Bond_strengt

h_between_reinforcement_and_self-compacting_concrete/links/5432b87c0cf225bddcc7c7b8.pdf [Accessed 30 Apr. 2019].

Solidia Technologies (2018). *White Paper on Water Use by Global Cement and Concrete Industry Finds Potential Savings Approaching Two Billion Tons of Water Per Year*. [online] Piscataway: Solidia Technologies, p.1. Available at: http://solidiatech.com/wp-content/uploads/2014/04/Solidia-Water-White-Paper-News-Release-April-2014-FINAL.pdf [Accessed 13 Nov. 2018].

Tweedie, N. (2018). Is the world running out of sand? The truth behind stolen beaches and dredged islands. *The Guardian*. [online] Available at: https://www.theguardian.com/global/2018/jul/01/riddle-of-the-sands-the-truth-behind-stolen-beaches-and-dredged-islands [Accessed 13 Nov. 2018].

WWAP (United Nations World Water Assessment Programme). 2018. The United Nations World Water Development Report 2018: Nature-based Solutions. Paris, UNESCO.

Appendices are available as 'supplementary files' (please see download area)